JPE 16-3-22

http://dx.doi.org/10.6113/JPE.2016.16.3.1046
ISSN(Print): 1598-2092 / ISSN(Online): 2093-4718

Mitigation of Negative Impedance Instabilities in a DC/DC Buck–Boost Converter with Composite Load

Suresh Singh[†], Nupur Rathore[*], and Deepak Fulwani[*]

[†,*]Department of Electrical Engineering, Indian Institute of Technology Jodhpur, Jodhpur, India

Abstract

A controller to mitigate the destabilizing effect of constant power load (CPL) is proposed for a DC/DC buck–boost converter. The load profile has been considered to be predominantly of CPL type. The negative incremental resistance of the CPL tends to destabilize the feeder system, which may be an input filter or another DC/DC converter. The proposed sliding mode controller aims to ensure system stability under the dominance of CPL. The effectiveness of the controller has been validated through real-time simulation studies and experiments under various operating conditions. The controller has been demonstrated to be robust with respect to variations in supply voltage and load and capable of mitigating instabilities induced by CPL. Furthermore, the controller has been validated using all possible load profiles, which may arise in modern-day DC-distributed power systems.

Key words: Composite load, Constant power load, DC/DC buck–boost converter, Negative impedance instabilities, Sliding mode control, Voltage regulation

I. INTRODUCTION

Advancements in the power electronics technology have been a key factor in the development of modern-day power systems, including renewable source-based microgrids, vehicular power systems, and data center power systems [1], [2]. Given the intensive use of power electronic converters, these systems are usually referred to as multiconverter power distribution systems or DC-distributed power systems [3]. Power electronic converters in such systems are tightly regulated to improve system performance and form a cascaded architecture. These tightly regulated converters exhibit negative incremental impedance and behave as constant power loads (CPLs). These converters also tend to destabilize the supply system, which may be an input filter or another DC/DC converter [4], [5]. The CPL-induced negative impedance instability in buck, boost, and buck–boost converters in continuous conduction mode (CCM) and discontinuous conduction mode (DCM) under voltage-mode and current-mode controls has been analyzed in [6]. All converters loaded by CPL and operating in CCM are unstable under both control modes. The operation of converters in DCM with CPLs is not much of a challenge from a stability point of view; control design in such cases translates to linear control system design, which is similar to control design with resistive load [6], [7]. In particular, controlling boost and buck–boost converters with CPL becomes more challenging as they are unstable even with resistive load given their non-minimum phase structure [2].

Authors in [8] have presented a controllability analysis of nonlinear switched systems composed of DC/DC converters with CPL using the differential geometry-based approach and concluded that DC/DC converters loaded with CPL can be controlled. Many techniques have been proposed by researchers to compensate the CPL effect. A method based on active damping has been presented in [9] to compensate the CPL effect in DC/DC converters. In active damping, virtual resistance is emulated in series with the inductor, which stabilizes the system as a result of increased system damping. The amount of CPL that can be compensated using this method is limited, and an assessment of system stability in the small-signal sense is performed. The use of nonlinear feedback to cancel out nonlinearity attributed to CPL and to stabilize the system is presented in [3]. This technique is termed as loop cancellation or feedback linearization and can be used to compensate any amount of CPL. Poor noise immunity attributed to the use of a differentiator is a major drawback of the loop cancellation technique. The pulse adjustment technique, in which the regulation of converter

Manuscript received Feb. 8, 2015; accepted Dec. 9, 2015
Recommended for publication by Associate Editor Se-Kyo Chung.
[†]Corresponding Author: sureshkumar@iitj.ac.in
Tel: +91 291 244 9051, Indian Institute of Technology Jodhpur
[*]Dept. of Electrical Eng., Indian Institute of Technology Jodhpur, India

output voltage is achieved by transmitting high and low power pulses rather than PWM, is proposed in [1], [4] to stabilize a buck–boost converter loaded with a combination of CPL and resistive load. A modified version of the pulse adjustment technique to handle variation in the input supply using variable high-power pulses is presented in [10], considering a buck–boost converter loaded by CPL. An amplitude death solution based on coupling-induced stabilization is presented in [11] for open-loop stabilization of CPL-loaded buck converters.

Nonlinear control-based methods that compensate the CPL effect in DC/DC converters and DC-distributed power systems in general are more appealing as they offer more robustness and global stability analysis, avoiding the limitations of the controller designed through linear methods. Nonlinear passivity-based controllers (PBCs) have been proposed in [12] for DC/DC converters loaded by CPL. The proposed method results in a linear PD controller for buck converter and nonlinear PD controller for boost and buck–boost converters, which may be transformed into the equivalent linear PD control. High noise sensitivity is a major concern in controllers designed through the PBC approach because of the use of a differentiator. Among the nonlinear control schemes, sliding mode control (SMC), a subclass of variable structure control, has been one of the preferred choices to control linear/nonlinear switched power electronic systems, among its many other applications. Controllers designed through the nonlinear SMC approach are robust to system parameter variations and external disturbances, are simple to implement, and offer global stability analysis [13]. For detailed information on the theory of SMC and its prominent features, see [14] and references therein. Authors in [15] have presented a unified approach to design PWM-based SMCs for DC/DC converters with resistive load and operating in CCM, wherein the switching function is in PID form. The control of a buck–boost converter with resistive load using the simple switching function in the current and voltage modes is presented in [16] and [17], respectively. A PWM-based SMC for a buck–boost converter with resistive load is proposed in [18], wherein the ideal sliding mode is generated in an auxiliary observer loop to prevent the chattering phenomenon. The boundary control with sliding mode using the first-order switching function having negative slopes has been presented to mitigate the CPL effect in boost and buck–boost converters in [2].

In light of modern DC-distributed power systems having renewable energy sources, storage units with sophisticated charge controllers, and tightly regulated cascaded converters, the presence of composite loads consisting of constant resistance, constant current, and CPL components is inevitable. In a modern-day scenario, DC/DC converters have to supply the aforementioned load profile and ensure high-quality power supply to sophisticated loads.

This study presents a robust SMC design for an inverted topology DC/DC buck–boost converter operating in CCM and feeding a composite load, which is dominated by CPL. The selected switching function of the controller that ensures the mitigation of the CPL caused instabilities and tight regulation of the converter output voltage under different operating conditions. The proposed controller ensures system operation at a constant switching frequency and avoids the limitations of the conventional SMC. A condition for system stability has been established, and the performance of the proposed controller has been validated through real-time simulation studies and experimental results. The controller is robust for sufficiently large step changes in the input voltage and load.

The remainder of the paper is organized as follows: In Section II, a model of the inverted topology DC/DC buck–boost converter supplying a composite load is presented. In Section III, a PWM-based sliding mode controller is proposed, wherein the existence of a sliding mode and the stability of the switching function are proven. Results and discussion are presented in Section IV, and the conclusion is given in Section V.

II. System Modeling

As mentioned in the previous section, the system under consideration is a DC/DC buck–boost converter supplying power to a composite load profile (Fig. 1). The converter is expected to regulate its output voltage at a desired level, which may be lower or higher than its input voltage depending on the mode of converter operation (buck or boost). The input source of the converter may be the output of a rectifier unit or the output of an MPPT converter in the case where the power comes from a renewable energy source, such as solar PV or wind turbine. The load profile is a composite having constant resistance, constant current, and constant power components. This assumption addresses the need of present-day DC-distributed power systems to supply power to different load profiles. For example, storage batteries in an AC/DC microgrid behave as constant current load under constant current charging mode, and tightly regulated point-of-load converters in the multiconverter power distribution system behave as CPLs. Conventional constant resistance DC loads have been relatively common in DC power systems for centuries and are still relevant today.

The nonlinear state space averaged model of the system shown in Fig. 1 can be represented by the following mathematical models:

$$L\frac{di_L}{dt} = uE + (1-u)v_C, \tag{1a}$$

$$C\frac{dv_C}{dt} = -(1-u)i_L - i_{load}, \tag{1b}$$

where inductor current i_L and capacitor voltage v_C are the state variables of the system; E is the input voltage; L and C

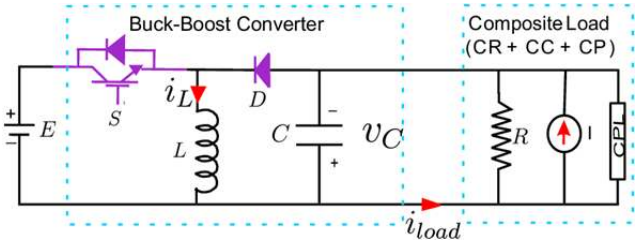

Fig. 1. Buck–boost DC/DC converter supplying a composite load.

are the converter inductor and capacitor, respectively; and $u \in \{0,1\}$ is the control input. Modeling of the CPL also constrains the values of i_L and v_C. Furthermore, i_L and $v_C \in \Omega$, where set Ω is a subset of R^2, that is,

$$i_L, v_C \in \Omega \subseteq R^2 \backslash \{0\}. \quad (2)$$

Furthermore, the load current i_{load} drawn by the composite load is expressed as follows:

$$i_{load} = \frac{v_C}{R} + I_{const} + \frac{P}{v_C}; v_C > 0, \quad (3)$$

where P is the rated power of the CPL and v_C is the output voltage of the converter or the voltage at the load terminals. The load current i_{load} has three components, namely, current drawn by resistive component R, constant current component I_{const}, and current drawn by the CPL component $\frac{P}{v_C}$. The ideal model of the buck–boost converter (1) was considered so that the destabilizing effect of the CPL will be as pronounced as possible. In practical converters, the presence of dissipative elements, such as switch resistance, diode resistance, inductor, and capacitor ESRs, increases natural damping of the system, which reduces the severity of the CPL-induced instability effect [11].

III. Sliding Mode Control Design

A. Switching Function

This section proposes a sliding mode controller for the nonlinear model of the DC/DC buck–boost converter system defined in (1). The first step in the design of a sliding mode controller for a given system is to design a stable switching function that meets system requirements. The proposed switching function is expressed as follows:

$$s := \beta_1(i_L - i_{Lref}) + \beta_2(v_C - v_{Cref}) + \beta_3 \int (v_C - v_{Cref})dt, \quad (4)$$

where i_{Lref} and v_{Cref} are the reference values of i_L and v_C, respectively. β_1, β_2, and β_3 are the constants that control the convergence speed of the switching function. The first term in the switching function expression given in (4) requires a reference inductor current, which depends on the input voltage and load. Therefore, obtaining the inductor current reference as the system input voltage is difficult and the load is subjected to changes. We use a high-pass filter (HPF) to overcome the estimation problem of the inductor current reference. High-pass filtered inductor current has been used to compute inductor current errors $(i_L - i_{Lref})$ [19], [20].

In the steady state, the inductor current error must be zero; therefore, a nonzero value switching function would indicate a steady-state error in the voltage in the absence of the last term. The last term of the switching function ensures zero steady-state error in the output voltage [20].

B. PWM-based Control Law

To compute the control law $u(t)$ for the PWM-based sliding controller, the following reaching dynamics is used:

$$\dot{s} := -\lambda s - Qsgn(s), \quad (5)$$

where $\lambda > 0$ and $Q > 0$ are additional tuning parameters used to control convergence speed. Using (1), (4), and (5) and solving $u(t)$ results in the following equation of the instantaneous converter duty cycle in terms of the state variables and converter parameters:

$$u(t) = \frac{\frac{\beta_2}{C} i_L + \frac{\beta_2}{C} i_{load} - \frac{\beta_1}{L} v_C - \beta_3 (v_C - v_{Cref}) - \lambda s - Qsgn(s)}{\frac{\beta_1}{L} E - \frac{\beta_1}{L} v_C + \frac{\beta_2}{C} i_L}. \quad (6)$$

The expression of the instantaneous duty cycle of converter $u(t)$ can be decomposed into two components, namely, equivalent control u_{eq} and discontinuous control u_N, which ensures robustness and implies that:

$$u(t) = u_{eq} + u_N. \quad (7)$$

The equivalent control u_{eq} is the control that acts on the system under sliding mode and is a representation of the switching control law of the conventional SMC. The discontinuous component u_N provides robustness against parameter uncertainties and external disturbances.

C. Existence of the Sliding Mode

Trajectory starting from any initial condition must reach the sliding surface in finite time and must be constrained to the surface afterward. The control law should be designed to ensure reachability conditions. The existence of the sliding mode for the proposed PWM-based sliding mode controller (6) is proven based on the reaching dynamics given in [14], as follows:

The reaching dynamics:

$$\dot{s} = -\lambda s - Qsgn(s). \quad (8)$$

The values of λ and Q are greater than zero, which ensure that the reachability condition:

$$s^T \dot{s} < -\eta |s| \quad (9)$$

is satisfied for $\eta > 0$.

Now, considering the reaching dynamics of (8), the left-hand side of the reachability condition $s^T \dot{s}$ becomes:

$$s^T \dot{s} = s^T [-\lambda s - Qsgn(s)], \quad (10)$$

which implies that:

$$s^T \dot{s} = [-\lambda s^2 - Q|s|] \text{ (because } s^T s = |s|^2), \quad (11)$$

where $Q > 0$ and $\lambda > 0$. Therefore,

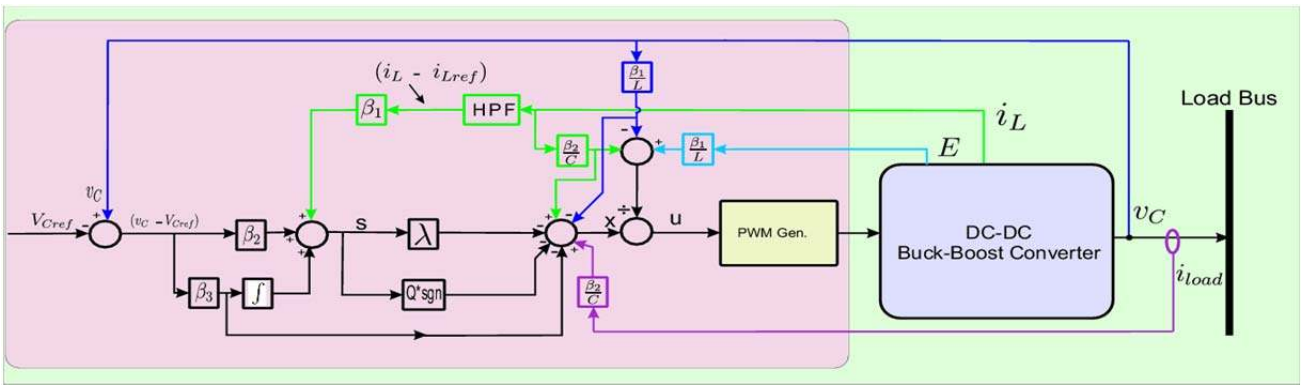

Fig. 2. Proposed sliding mode control scheme for the buck–boost converter system.

$$s^T\dot{s} = -|s|[\lambda|s| + Q], \tag{12}$$

which implies that:

$$s^T\dot{s} < -\eta|s|, \tag{13}$$

for all $\eta \geq \lambda|s| + Q$. This completes the proof.

D. Stability of the System at the Switching Surface s = 0

The existence of the sliding mode proven in the previous section implies that $s = 0$ would be attained in finite time. The trajectory after reaching the switching surface $s = 0$ must converge to the desired operating point along the switching surface to ensure system stability. That is,

$$s \coloneqq \beta_1(i_L - i_{Lref}) + \beta_2(v_C - v_{Cref}) + \beta_3\int (v_C - v_{Cref})dt = 0 \tag{14}$$

The reduced-order system dynamics during the sliding mode is expressed as follows:

$$i_L = -\frac{\beta_2}{\beta_1}(v_C - v_{Cref}) - \frac{\beta_3}{\beta_1}\int (v_C - v_{Cref})dt + i_{Lref}, \tag{15a}$$

$$C\frac{dv_C}{dt} = -(1-u)i_L - i_{load}. \tag{15b}$$

Eliminating i_L, the reduced-order dynamic model becomes:

$$C\frac{dv_C}{dt} - \frac{\beta_2}{\beta_1}(1-u)(v_C - v_{Cref}) - \frac{\beta_3}{\beta_1}(1-u)\int (v_C - v_{Cref})\,dt + (1-u)i_{Lref} + i_{load} = 0, \tag{16}$$

Differentiating (16) with respect to time, the expression becomes:

$$C\frac{d^2v_C}{dt^2} - \frac{\beta_2}{\beta_1}(1-u)\frac{dv_C}{dt} - \frac{\beta_3}{\beta_1}(1-u)(v_C - v_{Cref}) + \frac{di_{load}}{dt} = 0. \tag{17}$$

By expending the derivative of load current $i_{load}(v_C)$ using Taylor's series, we can define:

$$\frac{di_{load}}{dt} = \frac{\partial i_{load}}{\partial v_C}\frac{\partial v_C}{dt} + \delta(v_C), \tag{18}$$

where $\delta(v_C)$ represents all higher-order terms. We let $||\delta(v_C)|| \leq \delta_1$ and $||\dot{\delta}(v_C)|| \leq \delta_2$, where δ_1 and $\delta_2 > 0$. Substituting (18) into (17) results in:

$$C\frac{d^2v_C}{dt^2} + \left[\frac{1}{R} - \frac{P}{v_C^2} - \frac{\beta_2}{\beta_1}(1-u) + \dot{\delta}(v_C)\right]\frac{dv_C}{dt} - \frac{\beta_3}{\beta_1}(1-u)v_C + \frac{\beta_3}{\beta_1}(1-u)v_{Cref} = 0 \tag{19}$$

or

$$C\frac{d^2v_C}{dt^2} + F_1\frac{dv_C}{dt} + F_2v_C + F_3 = 0, \tag{20a}$$

where:

$$F_1 = \frac{1}{R} - \frac{P}{v_C^2} - \frac{\beta_2}{\beta_1}(1-u) + \dot{\delta}(v_C), \tag{20b}$$

$$F_2 = -\frac{\beta_3}{\beta_1}(1-u), \tag{20c}$$

$$F_3 = \frac{\beta_3}{\beta_1}(1-u)v_{Cref}. \tag{20d}$$

In the previously presented equations, $||\dot{\delta}(v_C)|| \leq \delta_2$ is the derivative for all higher-order terms. Equation (20) describes the behavior of the closed-loop system on the switching surface $s = 0$. To ensure system stability on the switching surface, $s = 0$, the following conditions must be satisfied:

$$F_1 > 0, \tag{21a}$$

$$F_2 > 0. \tag{21b}$$

Considering that $\beta_1 = 1$, the nominal value of control input $u = U$, and the capacitor voltage $v_C = v_{Cref}$, the aforementioned conditions imply that:

$$\left[\frac{1}{R} - \frac{P}{v_{Cref}^2} - \beta_2(1-U) + \dot{\delta}(v_C)\right] > 0, \tag{22a}$$

$$-\beta_3(1-U) > 0. \tag{22b}$$

Therefore, to ensure system stability with the given operating conditions and loading profile, the values of parameters β_2 and β_3 can be selected to satisfy the following conditions:

$$\beta_2 < \frac{1}{(1-U)}\left[\frac{1}{R} - \frac{P}{v_{Cref}^2} + \dot{\delta}(v_C)\right], \tag{23a}$$

$$\beta_3 < 0. \tag{23b}$$

Notably, the constant current component of the load does not in any way influence system stability.

IV. Results and Discussion

TABLE I
SIMULATION PARAMETERS

Parameter	Value	Symbol
Converter rating	1 kW	
Inductance	2 mH	L
Capacitance	47 µF	C
Constants	1, −50, −10,000	$\beta_1, \beta_2, \beta_3$
Constant	2,000	λ
Constant	0.5	Q
Input voltage	220 V	E
Load resistance	100 Ω	R
CPL	200 W	P
Constant current load	0.5 A	I_{const}
HPF time constant	0.00015	τ
Switching frequency	25 kHz	f_s

Fig. 3. An image of the OPAL-RT digital simulator.

In this section, the performance of the proposed sliding mode controller is validated using real-time simulation studies and experiments on a laboratory prototype of the proposed buck–boost converter.

A. Real-Time Simulation Studies

The proposed SMC scheme for the DC/DC buck–boost converter system (Fig. 1) has been validated using real-time simulation. MATLAB/SIMULINK is used for system modeling, and real-time simulation is conducted using the OPAL-RT digital simulator. The buck and boost operating modes have been considered to validate controller performance in steady state and under dynamic changes in input voltage and load. Nominal values in system parameters and variables used in the real-time simulation are provided in Table I. Fig. 3 shows a picture of the OPAL-RT digital simulator used to perform real-time simulations.

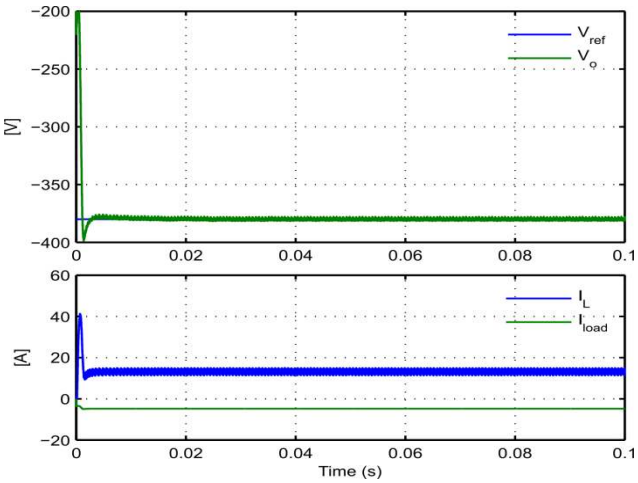

Fig. 4. Boost mode: start-up and steady-state response.

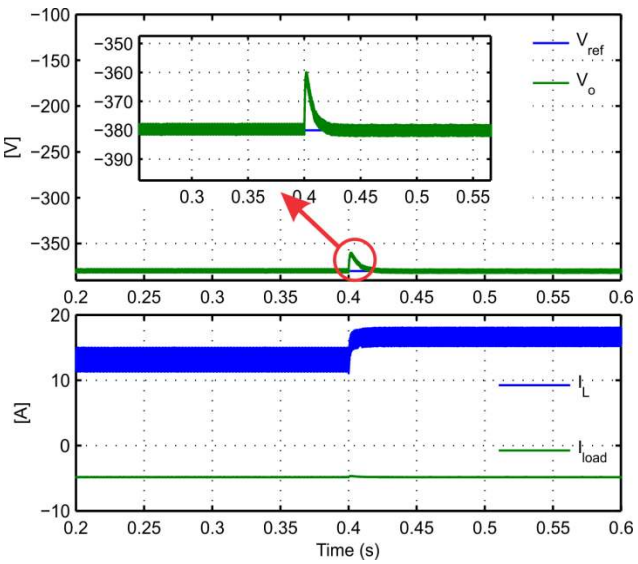

Fig. 5. Boost mode: transient response corresponding to 30% decrease in E at $t = 0.4$ s.

B. Boost Mode

In boost mode, the converter is controlled to provide a regulated output voltage of −380 V. The results of the real-time simulation in boost mode are shown in Figs. 4–7. Fig. 4 shows that the converter output voltage and inductor current reach their references in less than 4 ms and retain their values thereafter. The steady-state error in the voltage is zero, which is further confirmed in the zoomed plot shown in Fig. 5. The figure also shows the transient response with respect to 30% reduction in the input voltage. The output voltage decreases by approximately 10 V and returns to its steady-state value in <0.020 s. The inductor current instantly tracks its new reference and the load current remains constant because of no load changes. Figs. 6 and 7 show the transient response with respect to 100% increase in constant current and constant power component of the load at $t = 0.8$ s and

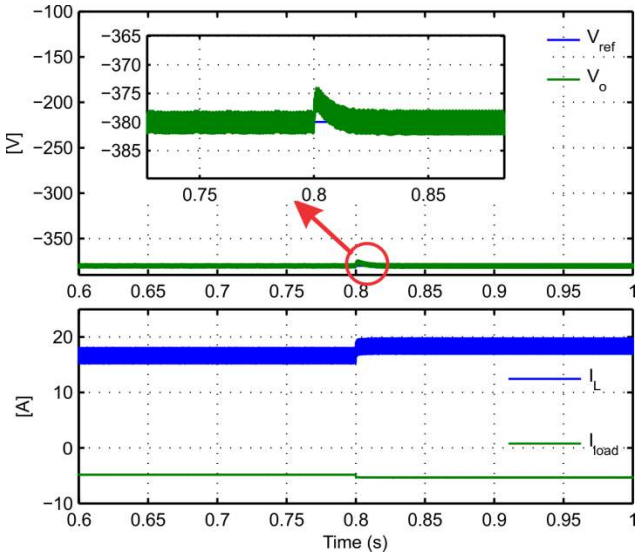

Fig. 6. Boost mode: transient response corresponding to 100% increase in I_{const} at $t = 0.8$ s.

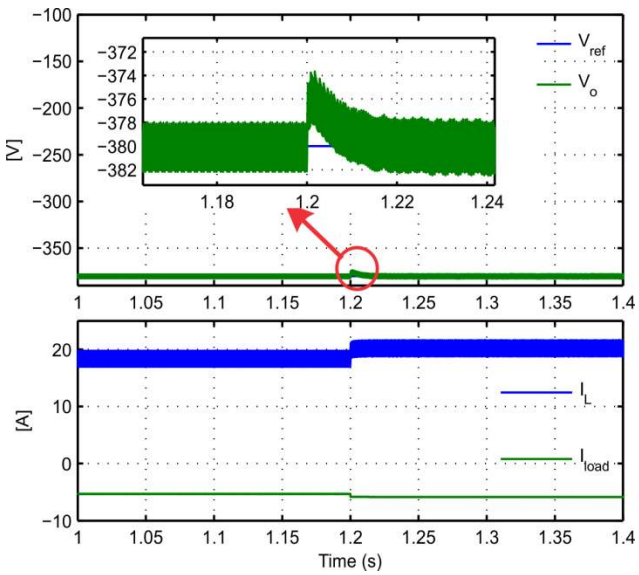

Fig. 7. Boost mode: transient response corresponding to 100% increase in P at $t = 1.2$ s.

$t = 1.2$ s, respectively, maintaining a fixed resistive load. The output voltage is briefly reduced by 5 and 6 V in response to the step changes in constant current and CPL, respectively; the output voltage recovers to its steady-state value relatively fast. The inductor and load current instantly change and reflect the corresponding load changes.

C. Buck Mode

The performance of the proposed controller has also been validated in buck mode, wherein the buck–boost converter system is controlled to produce a regulated output voltage of −120 V. The voltage and current waveform in the steady state are shown in Fig. 8. Meanwhile, Figs. 9–11 show the transient performance with respect to the step changes in the

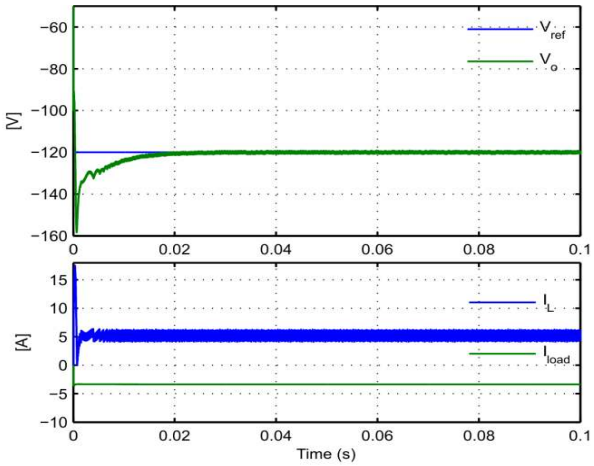

Fig. 8. Buck mode: start-up and steady-state response.

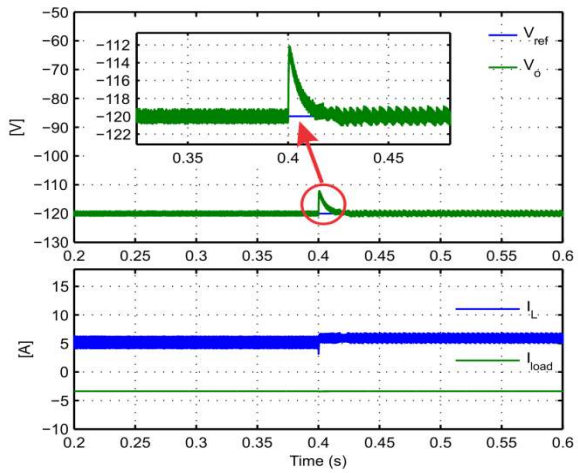

Fig. 9. Buck mode: transient response corresponding to 30% decrease in E at $t = 0.4$ s.

input voltage, constant current load, and CPL while maintaining a fixed resistive load.

Fig. 8 shows that the output voltage reaches a steady state in less than 20 ms with zero steady-state error. The values for the inductor current and load current are also retained. As shown in Fig. 9, in response to the 30% reduction in the input voltage at $t = 0.4$ s, the output voltage decreases by 8 V and returns to its steady-state value at less than $t = 0.025$ s.

Furthermore, the inductor current instantly tracks its changed reference, whereas the load current remains unchanged with no change in the load. The transients of a short duration are observed in the output voltage in the range of 4 V when the constant current load increases by 100% (Fig. 10). The output voltage clearly returns to its steady-state value in less than 0.010 s; moreover, the inductor and load currents instantly change to reflect the increase in load.

The voltage and current waveforms corresponding to the 100% step increase in CPL are shown in Fig. 11. An impulse transient of $< \pm 10$ V can be observed in the output voltage, in which the controller sufficiently handles and forces the

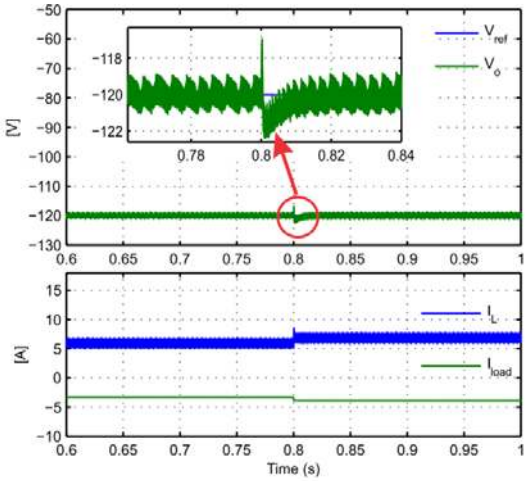

Fig. 10. Buck mode: transient response corresponding to 100% increase in I_{const} at t = 0.8 s.

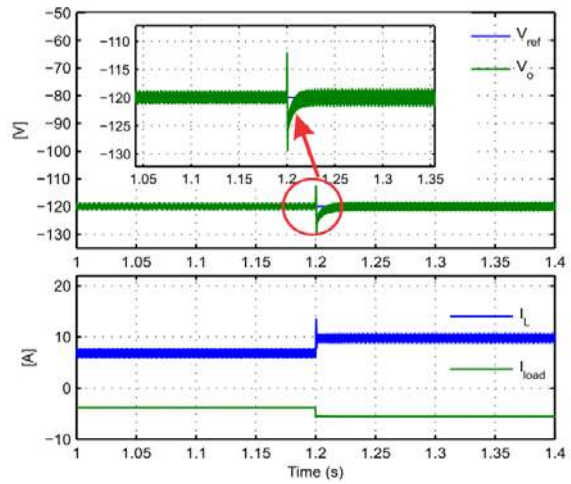

Fig. 11. Buck mode: transient response corresponding to 100% increase in P at t = 1.2 s.

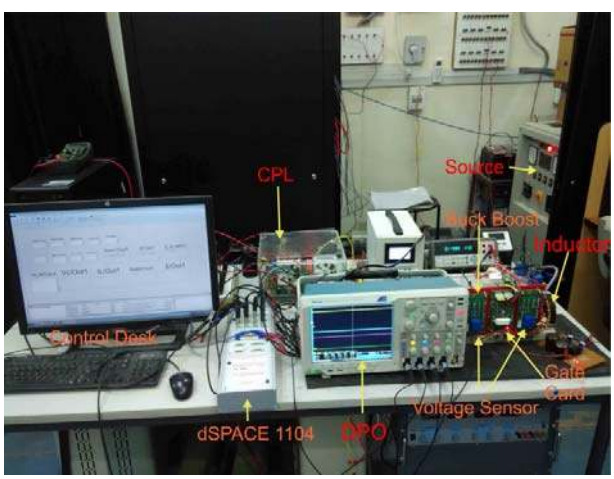

Fig. 12. An image of the experimental setup.

output voltage to its steady-state value. The inductor current in this case shows an overshoot at the step change instance, but tracks its changed reference instantly. The load current also reflects the corresponding load change.

D. Experimental Validation

The controller is implemented using a dSPACE DS1104 controller board to validate the performance of the proposed sliding mode controller. The dSPACE controller board uses the MATLAB/SIMULINK environment for programming. DS1104 is specifically designed for the development of high-speed multivariable digital controllers and real-time simulations in various fields. DS1104 is a complete real-time control system based on a 603 PowerPC floating-point processor running at 250 MHz. For advanced I/O purposes, the board includes a slave DSP subsystem based on the TMS320F240 DSP microcontroller. The switching time period was 15×10^{-6} s. An image of the experimental setup is presented in Fig. 12.

The parameters of the converter were the same as that provided in Table I, and the selected controller parameters were $\beta_1 = 1$, $\beta_2 = -0.0192$, $\beta_3 = 5 \times 10^{-6}$, $\lambda = 20{,}000$, and $Q = 1$.

The experimental results under boost and buck modes under various operating conditions are shown in Figs. 13 and 14, respectively.

The experimental results under boost mode are shown in Fig. 13 with a nominal load of $R = 300\ \Omega$, $P = 200$ W, and $I_{const} = 0.5$ A. The value of resistive load in this experiment was kept at $300\ \Omega$ instead of $100\ \Omega$ because of unavailable suitable load to dissipate the required power at 380 V. Fig. 13 shows the results corresponding to the following steady-state conditions: when E is reduced to 150 V, when I_{const} is increased to 1 A, and when CPL power P is increased to 400 W. In all cases, the controller ensures system stability and tightly regulates the output voltage.

Fig. 14 shows the experimental results under buck mode. In this case, the load profile was the same as that in the simulation studies. Fig. 14(a) shows the experimental results in steady-state, whereas Figs. 14(b), 14(c), and 14(d) show the transient performance corresponding to variations in input voltage, constant current component of the load, and CPL power, respectively. Based on the plots, the controller ensures that the desired output voltage is reached and is robust to sufficiently large variations in the input voltage and load.

Thus, the real-time simulation studies and experimental results presented previously validate the performance of the proposed sliding mode controller in boost and buck modes under various operating conditions. The controller is able to mitigate instabilities given the presence of the dominant CPL component and tightly regulates the output voltage with zero steady-state error. The controller has been observed to be robust with respect to the changes in input voltage, constant current load, and CPL. The effectiveness of the proposed controller has been validated with realistic composite load profiles.

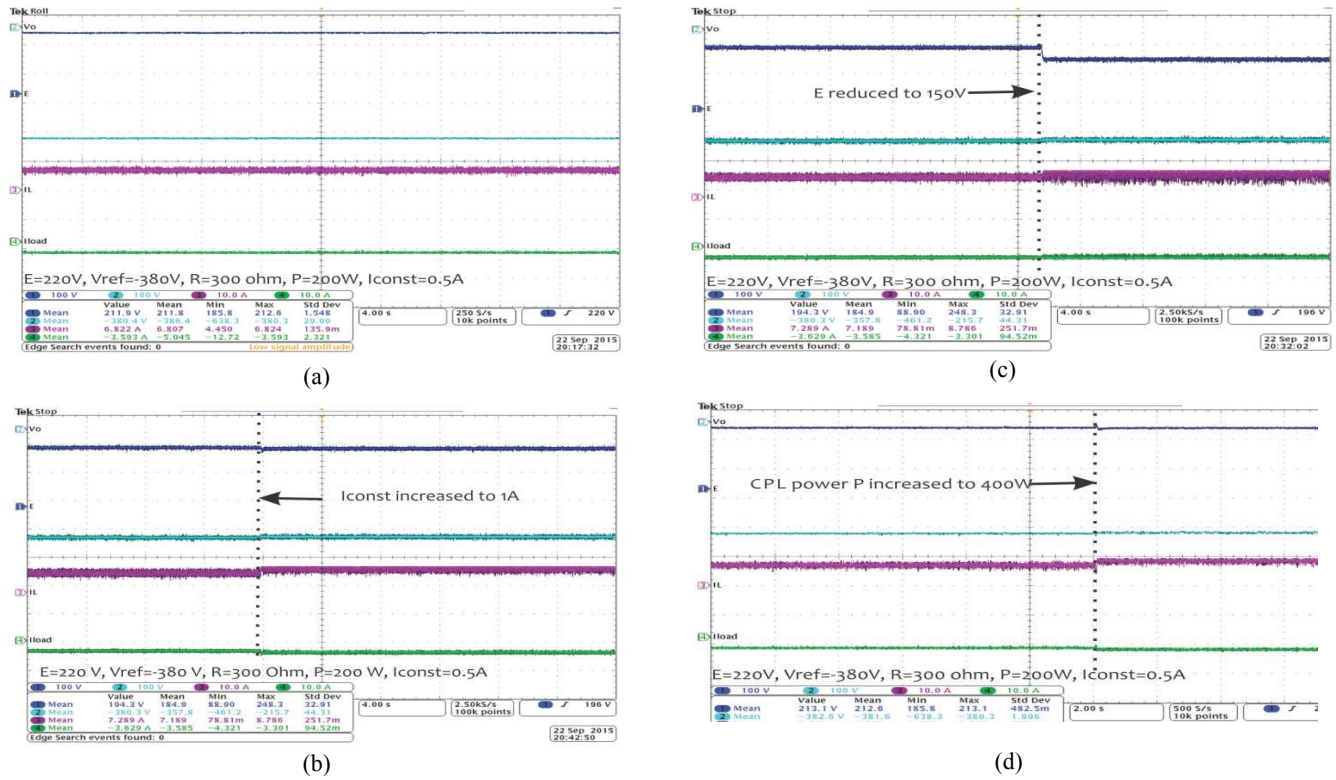

Fig. 13. Experimental results under boost mode: (a) steady-state response; (b) transient response when E is reduced to 150 V; (c) transient response when I_{const} is doubled; and (d) transient response when CPL power P is doubled.

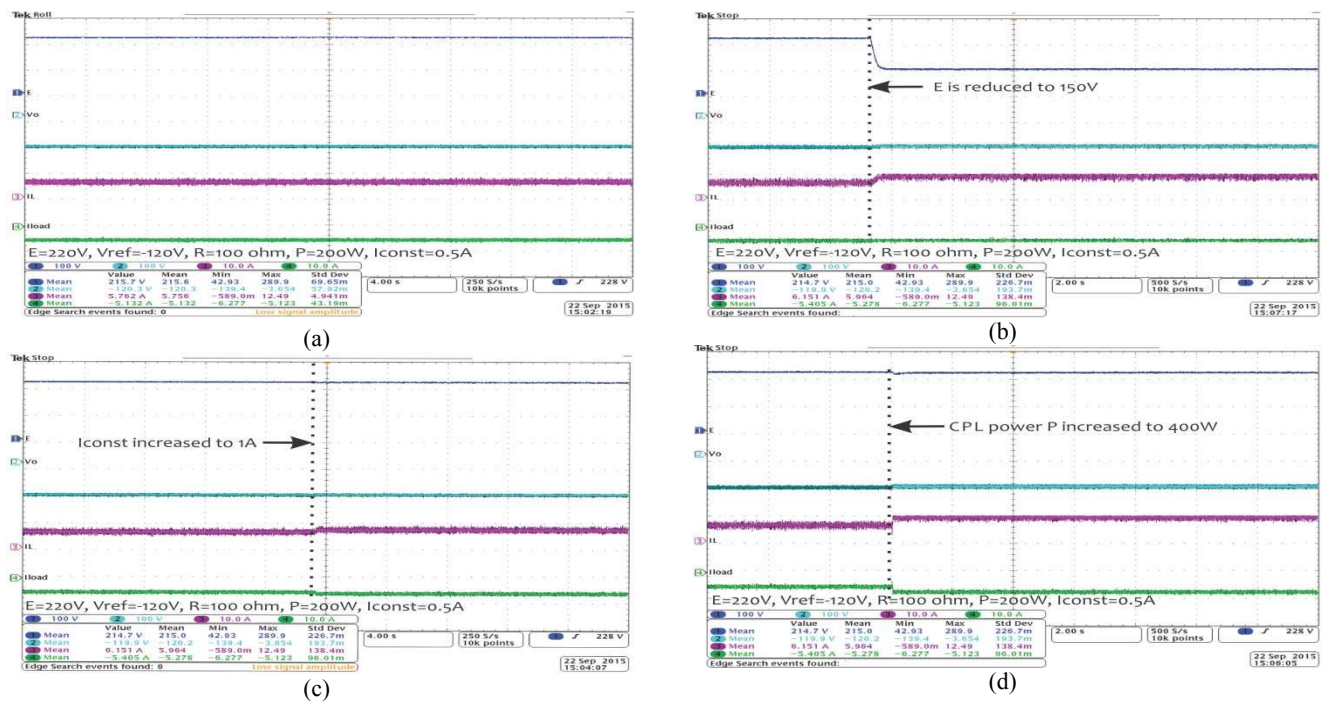

Fig. 14. Experimental results under buck mode: (a) steady-state response; (b) transient response when E is reduced to 150 V; (c) transient response when I_{const} is doubled; and (d) transient response when CPL power P is doubled.

V. CONCLUSION

A robust sliding mode controller has been proposed for a DC/DC buck–boost converter supplying a composite load. The proposed controller ensures mitigation of negative impedance instabilities under the dominance of CPL. The existence of sliding mode and system stability has been proven. The buck and boost operating modes have been

considered, wherein the converter is responsible for maintaining its output voltage at the desired level. Real-time simulation studies and experimental results have been presented to validate the effectiveness of the proposed controller under various operating conditions. The controller has been observed to be robust with respect to variations in supply voltage and load.

ACKNOWLEDGMENT

The authors would like to thank the Ministry of New and Renewable Energy, India for financially supporting this work under project no. S/MNRE/LC/20110007. The authors would also like to thank Mr. Vinod Kumar and Mr. Kumar Gaurav for their help in executing the hardware implementation.

REFERENCES

[1] A. Khaligh, A. M. Rahimi, and A. Emadi, "Negative impedance stabilizing pulse adjustment control technique for DC/DC converters operating in discontinuous conduction mode and driving constant power loads," *IEEE Trans. Veh. Technol.,* Vol. 56, No. 4, pp. 2005-2016, Jul. 2007.

[2] C. N. Onwuchekwa and A. Kwasinski, "Analysis of boundary control for boost and buck-boost converters in distributed power architectures with constant-power loads," in *26th Annual IEEE Applied Power Electronics Conference and Exposition(APEC),* pp. 1816-1823, 2011.

[3] A. M. Rahimi, G. A. Williamson, and A. Emadi, "Loop-cancellation technique: A novel nonlinear feedback to overcome the destabilizing effect of constant-power loads," *IEEE Trans. Veh. Technol.,* Vol. 59, No. 2, pp. 650-661, Feb. 2010.

[4] A. Khaligh, A. M. Rahimi, A. Chakraborty, and A. Emadi, "Analysis and stabilization of a Buck-Boost DC-DC converter feeding constant power loads in parallel with conventional loads in vehicular systems," in *32nd Annual Conference on IEEE Industrial Electronics(IECON)*, pp. 2799-2804, 2006.

[5] S. Singh, D. Fulwani, and V. Kumar, "Robust sliding-mode control of dc/dc boost converter feeding a constant power load," *IET Power Electron.,* Vol.8, No.7, pp.1230-1237, Jul. 2015.

[6] S. C. Smithson and S. S. Williamson, "Constant power loads in more electric vehicles-an overview," in *38th Annual Conference on IEEE Industrial Electronics Society (IECON)*, pp. 2914-2922, 2012.

[7] A. M. Rahimi and A. Emadi, "Discontinuous-conduction mode DC/DC converters feeding constant-power loads," *IEEE Trans. Ind. Electron.,* Vol. 57, No. 4, pp. 1318-1329, Apr. 2010.

[8] Z.-Y. Xu, Y.-L. Yu, W.-S. Xu, and Q.-D. Wu, "Controllability of nonisolated DC-DC converters with constant-power-load," in *24th Chinese Control and Decision Conference(CCDC),* pp. 669-673, 2012.

[9] A. M. Rahimi and A. Emadi, "Active damping in dc/dc power electronic converters: a novel method to overcome the problems of constant power loads," *IEEE Trans. Ind. Electron.,* Vol. 56, No. 5, pp. 1428-1439, May 2009.

[10] A. Khaligh, A. M. Rahimi, and A. Emadi, "Modified pulse-adjustment technique to control dc/dc converters driving variable constant-power loads," *IEEE Trans. Ind. Electron.,* Vol. 55, No. 3, pp. 1133-1146, Mar. 2008.

[11] S. R. Huddy and J. Skufca, "Amplitude death solutions for stabilization of dc microgrids with instantaneous constant-power loads," *IEEE Trans. Power Electron.,* Vol. 28, No. 1, pp. 247-253, Jan. 2013.

[12] A. Kwasinski and P. T. Krein, "Stabilization of constant power loads in dc-dc converters using passivity-based control," in *29th International Telecommunications Energy Conference(INTELEC)*, pp. 867-874, 2007.

[13] Y. He, W. Xu, and Y. Cheng, "A novel scheme for sliding-mode control of DC-DC converters with a constant frequency based on the averaging model," *Journal of Power Electronics*, Vol. 10, No. 1, pp. 1-8, Jan. 2010.

[14] J. Y. Hung, W. Gao, and J. C. Hung, "Variable structure control: a survey," *IEEE Trans. Ind. Electron.,* Vol. 40, No. 1, pp. 2-22, Feb. 1993.

[15] S.-C. Tan, Y. M. Lai, and C. K. Tse, "A unified approach to the design of PWM-based sliding-mode voltage controllers for basic DC-DC converters in continuous conduction mode," *IEEE Trans. Circuits Syst. I, Reg. Papers,* Vol. 53, No. 8, pp. 1816-1827, Aug. 2006.

[16] P. Salazar, P. Ayala, S. G. Jimenez, and A. F. Correa, "Design of a sliding mode control for a DC-to-DC buck-boost converter," in *25th Chinese Control and Decision Conference(CCDC),* pp. 4661-4666, 2013.

[17] P. Singh and S. Purwar, "Sliding mode controller for PWM based buck-boost DC/DC converter as state space averaging method in continuous conduction mode," in *2nd International Conference on Power, Control and Embedded Systems(ICPCES),* pp. 1-5, 2012.

[18] H. E. Fadil and F. Giri, "Reducing chattering phenomenon in sliding mode control of buck-boost power converters," in *International Symposium on Industrial Electronics (ISIE),* pp. 287-292, 2008.

[19] E. Santi, A. Monti, D. Li, K. Proddutur, and R. A. Dougal, "Synergetic control for DC-DC boost converter: implementation options," *IEEE Trans. Ind. Appl.,* Vol. 39, No. 6, pp.1803-1813, Nov./Dec. 2003.

[20] P. Mattavelli, L. Rossetto, G. Spiazzi, and P. Tenti, "General-purpose sliding-mode controller for DC/DC converter applications," in *24th Annual IEEE Power Electronics Specialists Conference(PESC)*, pp. 609-615, 1993.

Suresh Singh received his B.Tech. degree in Electrical Engineering from the Institute of Engineering and Technology, M.J.P. Rohilkhand University, Bareilly, India in 2000 and M.Tech. degree in Electrical Engineering from the Indian Institute of Technology Roorkee, Roorkee, India in 2003. He has seven years of teaching experience in different private technical institutions. He is currently working toward his Ph.D. in the area of Mitigation of Negative Impedance Instabilities in DC Microgrid, under the Department of Electrical Engineering at the Indian Institute of Technology Jodhpur, Jodhpur, India. His fields of interest include power electronics, power system dynamics and control, distributed generation, DC microgrids, and sliding mode control.

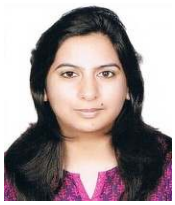

Nupur Rathore was born in Jodhpur, India. She received her B.E. degree in Electrical Engineering from M.B.M. Engineering College, Jodhpur, India in 2011 and M.Tech. degree in Energy from the Indian Institute of Technology (IIT), Jodhpur, India in 2013. She has been working toward her Ph.D. degree in Electrical Engineering from IIT Jodhpur since 2014. Her current research interests include DC/DC converters, control systems, sliding mode control, and DC microgrid.

Deepak Fulwani is working as an assistant professor in the Department of Electrical Engineering at the Indian Institute of Technology Jodhpur (IIT/J), Jodhpur, India. He also worked at IIT Guwahati and III Kharagpur. He obtained his Ph.D. degree from IIT Bombay in 2009. He was also awarded for his excellence in Ph.D. thesis work at the 48th convocation. His research fields include DC microgrid and network system control.